Studies of the interfacial structure of LaAlO₃ thin films on silicon by x-ray reflectivity and angle-resolved x-ray photoelectron spectroscopy

X. L. Li,[a] W. F. Xiang, H. B. Lu, and Z. H. Mai
Beijing National Laboratory for Condensed Matter Physics, Institute of Physics, Chinese Academy of Sciences, Beijing 100080, China

The microstructures of amorphous LaAlO₃ thin films deposited on silicon substrates by the laser molecular-beam epitaxy were studied by the x-ray reflectivity and the angle-resolved x-ray photoelectron spectroscopy. It was shown that the film/substrate interface contains a La-rich La$_x$Al$_y$O$_z$Si layer and a SiO$_x$ layer. It was shown that the electron density of the LaAlO₃ layer and the La$_x$Al$_y$O$_z$Si layer is not homogeneous along the growth direction due to the diffusion of La, Al, and Si. The growth kinetics of the LaAlO₃ film was described by three processes: (1) formation of the SiO$_x$ layer at the early stage whose thickness saturates rapidly at about 13 Å; (2) formation of the La$_x$Al$_y$O$_z$Si layer by the out diffusion of Si and the inner diffusion of La, Al (mostly La). This stage continues as the film grows (3) In the deposition process of LaAlO₃, the distributions of La and Al in the LaAlO₃ layer change from inhomogeneous to homogeneous. © *2005 American Institute of Physics*. [DOI: 10.1063/1.1941470]

I. INTRODUCTION

With the continuing miniaturization of the complementary metal-oxide semiconductor (CMOS) devices, high-k gate dielectrics have gained considerable attention to replace SiO₂ as the gate dielectric.[1] Candidate materials include Al₂O₃, Y₂O₃, La₂O₃, ZrO₂, HfO₂, and their pseudobinary oxides,[2–6] which are thermodynamically stable on silicon substrate.[7] LaAlO₃ as a compound of La₂O₃ and Al₂O₃ is considered as another most promising candidate. It has a steady interface with silicon and a higher dielectric constant of 25–27;[8] however, when these materials are deposited on silicon, SiO$_x$ or metal silicates are often formed at the interface.[9–12] The existence of these interfacial sublayers would reduce the overall electrical property. Understanding and controlling the growth of these interfacial sublayers are key to obtain high-performance high-k dielectric films.

Many authors have studied the interfacial structure of LaAlO₃ on silicon substrate by transmission electron microscopy (TEM), secondary-ion-mass spectroscopy (SIMS), and x-ray photoelectron spectroscopy (XPS).[13,14] The x-ray reflectivity has been considered an efficient and nondestructive tool to measure the microstructures of thin films such as the thickness, the electron-density profile, and the interfacial roughness of each layer in the film. In this article, the interfacial structure of the LaAlO₃ films was investigated by the x-ray reflectivity (XRR) technique and the angle-resolved XPS. The growth kinetics of LaAlO₃ film on Si substrate was discussed based on the results.

II. EXPERIMENTAL PROCEDURE

The LaAlO₃ films were deposited on n-type (100) Si substrates by the laser molecular-beam epitaxy (LMBE) technique.[15] Prior to the film deposition, Si wafers were cleaned with acetone, alcohol, and dilute HF solution to remove any native oxide layer, producing a hydrogen-terminated surface. The deposition was carried out at an oxygen pressure of 0.1 Pa and a substrate temperature of 700 °C. Three samples were prepared with different thickness of 50 Å (sample A), 80 Å (sample B), and 120 Å (sample C), respectively. High-resolution x-ray diffraction was performed to confirm that the LaAlO₃ films were amorphous.

The x-ray reflectivity and high-resolution x-ray-diffraction measurements were performed on a Bruker D8 Advance diffractometer at room temperature with Cu $K\alpha$ radiation. The incident beam was confined by a 0.1-mm slit 300 mm before the sample and the scattered beam was confined by a 0.2-mm slit. The angle-resolved XPS was performed on a PHI-5300/ESCA surface analysis system using Al $K\alpha$ ($h\nu$=1486.6 eV) at different takeoff angles. The position of the C1s peak was taken as a standard (with a banding energy of 285.0 eV).

III. RESULTS AND DISCUSSION

Shown in Fig. 1 are the x-ray reflectivity profiles of the three samples. We have tried to simulate the data by using the matrix method.[16,17] A simple two-slab model, which includes a LaAlO₃ layer and a SiO$_x$ interfacial layer on the silicon substrate, failed to reproduce the experimental data. The dashed lines in Fig. 1 are the best fit we can get with Bruker's LEPTOS program if a simple two-slab model is used. The large discrepancy between the simulations and the experiments enforced us to pursue a more complex model based on our XPS experiments.

The angle-resolved XPS analysis is performed on sample A to obtain the interfacial information about the film. The effective sampling depth, $Z=3\lambda \sin \theta$, is a function of the mean attenuation length, λ, and the takeoff angle, θ, of the photoelectrons. At a lower takeoff angle only the elec-
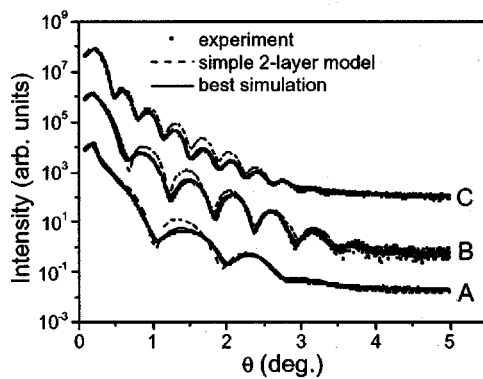
a)Electronic mail: bluelix1@163.com

FIG. 1. X-ray reflectivity spectra and theoretical simulations of the samples with different thickness, sample A: 50 Å, sample B: 80 Å, and sample C: 120 Å.

trons emitted from the near surface region are detected, and the signals are predominantly from the surface of the sample. While at a higher takeoff angle the signals contain the information of the sample interface. Figure 2(a) shows the La 3d core-level spectra of sample A at different takeoff angles of 15°, 30°, 45°, and 90°, respectively. One sees that the positions of the La $3d_{2/5}$ peaks at 834.9 eV are similar for the takeoff angles of 15°, 30°, and 45°. However, at the takeoff angle of 90° the peak of the La $3d_{5/2}$ is broader and shifts towards higher binding energy, consistent with the formation of La–O–Si bond.[18] Similar results of the Al 2p spectra are shown in Fig. 2(b). At the takeoff angle of 90° the peak position of the Al 2p shifts towards higher binding energy. It is clear from Fig. 2(b) that the peak profile of the Al 2p at the takeoff angle of 90° is composed of two peaks, one at 74.2 eV corresponding to the Al 2p in LaAlO₃ environment, another at 75.3 eV indicating the Al–O–Si bond at the interface. The peak at 75.3 eV disappears when the takeoff angle decreases. The La to Al ratios (La/Al) for different takeoff angles are estimated by the ratios of the La and Al peak areas in Figs. 2(a) and 2(b). The La to Al ratios (±2%) are 0.95, 0.98, 1.08, and 1.39 for the takeoff angles of 15°, 30°, 45°, and 90°, respectively. One can see that for the takeoff angles of 15°, 30°, and 45°, the La/Al ratios are very close to 1:1. However, at the takeoff angle of 90° the ratio of La/Al is greater than 1. A reasonable explanation is that the $La_xAl_yO_zSi$ layer contains high concentration of La. These results indicate that there is a La-rich $La_xAl_yO_zSi$ compound near the interface.

Figure 2(c) shows the angle-resolved Si 2s core-level spectra of sample A. The spectrum taken at 90° is composed of three peaks, noted as peaks I, II, and III, respectively. Peak III at 154.1 eV is attributed to SiO_x,[19] and peak II at 152.9 eV is related to $La_xAl_yO_zSi$ corresponding to the La–O–Si and Al–O–Si bonds. The intensity of peak III decreases with the decreasing takeoff angle and diminishes eventually at 30°. On the contrary, the intensity of peak II increases with the decreasing takeoff angle, indicating that the SiO_x layer lies below the $La_xAl_yO_zSi$ layer. Peak I at the binding energy of 150.4 eV is attributed to silicon. Its intensity decreases with the decreasing takeoff angle, but remains even at the
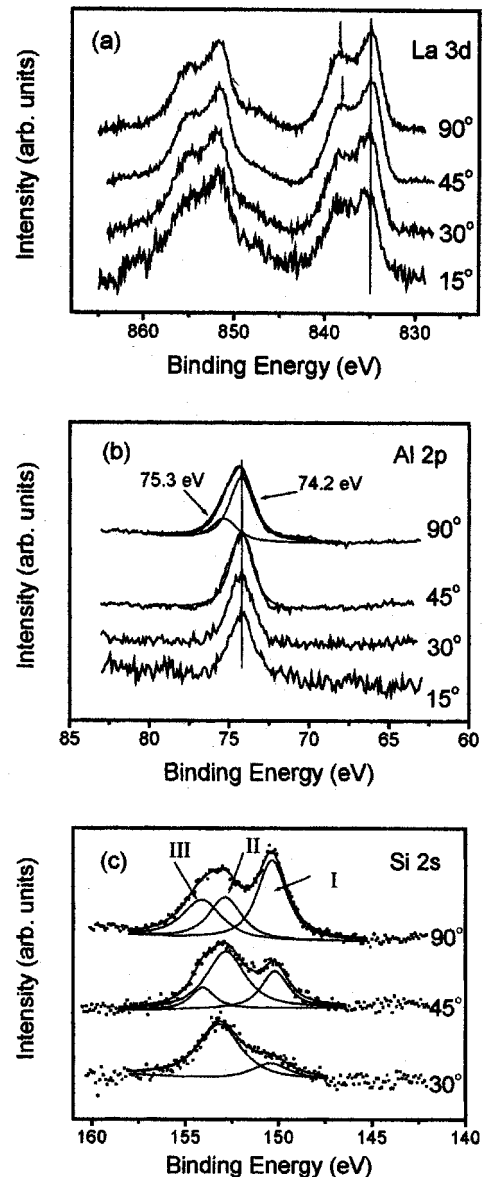

FIG. 2. (a) Angle-resolved spectra of the sample A's La 3d core level taken at the takeoff angles of 15° (surface sensitive), 30°, 45°, and 90°, (interface sensitive), respectivley. (b) Angle-resolved XPS spectra of sample A's Al 2p core level taken at the takeoff angles of 15°, 30°, 45°, and 90°, respectively. (c) XPS spectra of sample A's Si 2s core level taken at different takeoff angles of 30°, 45°, and 90°, respectively.

lowest takeoff angle of 30°. This may be due to the photo-electric signal from the edge of the Si substrate.

The XPS measurements of sample A indicate that there are a $La_xAl_yO_zSi$ component and a SiO_x component near the interface of $LaAlO_3$ and Si; the SiO_x layer lies below the $La_xAl_yO_zSi$ layer. Since the only difference between the three samples is the deposition time, it is reasonable to consider that samples B and C have a similar interfacial structure as sample A. Based on these results, we have used a three-layer model, which includes a $LaAlO_3$ layer, a $La_xAl_yO_zSi$ diffusion layer, and a SiO_x layer on top of the silicon substrate to fit the XRR spectra of the three samples in Fig. 1. For a better fitting the SiO_x layer is divided into two sublayers with a low electron-density layer and a high one. The low electron-density layer corresponds to the amorphous SiO_2

TABLE I. Parameters used in fitting the x-ray reflection curves: ρ is the electron density $(e^-/\text{Å}^3)\pm 0.01$, d is the layer thickness $(\text{Å})\pm 1$, and σ is the root-mean-square roughness of the interfaces $(\text{Å})\pm 0.5$.

	LaAlO_3 $\rho/d/\sigma$	Interface layer ($\rho/d/\sigma$)			Si substrate ρ/σ
		$\text{La}_x\text{Al}_y\text{O}_z\text{Si}$	SiO_x	Denser SiO_x	
Sample A	$1.27_{\text{Top}}-0.95_{\text{Bottom}}/44/2.8$	0.76/5/4.5	0.66/8/6	0.73/5/5	0.7/3
Sample B	$1.38_{\text{Top}}-1.10_{\text{Bottom}}/65/3.5$	0.77/10/9	0.66/9/5.5	0.74/5/5	0.7/3
Sample C	1.42/100/7.0	0.80/19/15	0.66/7/3	0.74/5/5	0.7/3

and the high one is believed to correspond to the quasiepitaxial growth of the SiO_2 near the substrate.[20,21] which is slightly denser than the Si substrate. Because there might exist suboxide at the SiO_2/Si interface,[22,23] we consider the SiO_x to be a better description of the interfacial SiO_2 layer. A linear gradient of LaAlO_3 compound density is also considered for samples A and B. The best simulation results are shown in Fig. 1. The parameters used in the simulation are listed in Table I. The electron-density profiles (EDPs) obtained from the simulation data are shown in Fig. 3.

The arrows in Fig. 3 indicate the interfaces of the $\text{LaAlO}_3/\text{La}_x\text{Al}_y\text{O}_z\text{Si}$, which are defined by the different density gradients of the two sides. The gradient of the $\text{La}_x\text{Al}_y\text{O}_z\text{Si}$ layer might be caused mostly by the out diffusion of Si, while that of the LaAlO_3 layer might be formed by the inner diffusion of La and Al (mostly La). From Table I, one can observe that the electron density of the LaAlO_3 layer of sample A is highly inhomogeneous and shows a graded distribution along the growth direction. It is about $1.27\ e^-/\text{Å}^3$ at the surface of the LaAlO_3 layer, and about $0.95\ e^-/\text{Å}^3$ in the vicinity of the substrate. It might be caused by the inhomogeneous depth distributions of La and Al in the LAO film. With the continuing increase of the thickness, the inhomogeneous is decreased gradually and the LaAlO_3 layer becomes more compact as the parameters of sample B showed. The electron density near the top surface of the LaAlO_3 layer is increased to $1.38\ e^-/\text{Å}^3$, and is about $1.10\ e^-/\text{Å}^3$ in the vicinity of the substrate. Eventually, the inhomogeneous of electron density disappeared. We can see from sample C that the electron density becomes homogeneous with a value of $1.42\ e^-/\text{Å}^3$. When the film is thicker, the La and Al in the LaAlO_3 layer would have enough time

to diffuse, hence the compositional grade of the LaAlO_3 layer is decreased gradually, and eventually the LaAlO_3 film becomes homogenous and compact.

It is impressive to find that the thickness of the $\text{La}_x\text{Al}_y\text{O}_z\text{Si}$ layer increases with the thickening of the LaAlO_3 layer, while the thickness of the SiO_x layer is basically changeless. We suggest that the oxygen diffusion occurs only at the early stage of the film growth, and the thickness of the SiO_x layer saturates at about 13 Å. It is in agreement with the previous study that the growth of SiO_x layer saturated with the time and the pressure but increased with the temperature in ZrO_2/Si system.[24] The diffusion of Si into LaAlO_3 layer is a dominant process of the interface growth mode.[25] The emission of Si towards the surface[26] during the growth promotes the formation of La–O–Si and Al–O–Si bonds (mostly La–O–Si bond as the XPS results of La-rich interface). Consequently, the thickness of the $\text{La}_x\text{Al}_y\text{O}_z\text{Si}$ layer increases. SiO generated at the interface of Si/SiO_2 via the reaction $\text{Si}+\text{SiO}_2\rightarrow\text{SiO}\uparrow$ is the most possible diffusion mode of the Si species.[27]

IV. CONCLUSIONS

The microstructures of amorphous LaAlO_3 thin films deposited on Si substrate were investigated by the x-ray reflectivity technique and the angle-resolved x-ray photoelectron spectroscopy. The results showed that there are a $\text{La}_x\text{Al}_y\text{O}_z\text{Si}$ compound and a SiO_x compound at the interface of LaAlO_3/Si substrate. The thickness of the SiO_x layer saturates rapidly at about 13 Å, while the thickness of the $\text{La}_x\text{Al}_y\text{O}_z\text{Si}$ layer keeps increasing as the deposition continues. The electron density of the LaAlO_3 layer is highly inhomogeneous along the growth direction. The gradient of the electron-density distribution decreases and disappears eventually as the LaAlO_3 layer becomes thick. From the discussion above, the growth kinetics of LaAlO_3 film grown on Si substrate can be described by the following three processes:

(1) At the early stage of the LaAlO_3 growth, oxygen atoms arrive easily at the Si substrate, the transport of oxygen should have a much higher diffusivity than oxygen diffusion at the growing SiO_x film, and the oxide growth is a rate-limiting step. At the following time, with the thickening of the SiO_x layer, the grown SiO_x prevents the further growth of SiO_x so that its thickness saturates rapidly.

(2) With the further deposition of LaAlO_3, the oxygen diffusion through the LaAlO_3 film becomes more difficult. Emission of Si species is the dominating diffusion mode
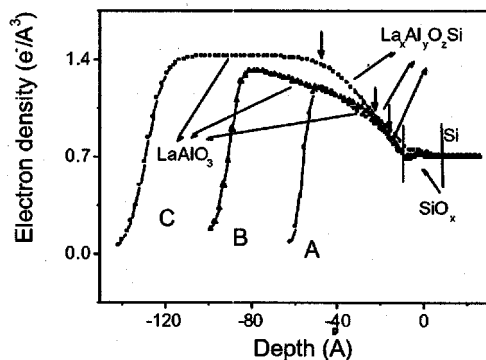

FIG. 3. Comparison of electron-density profiles (EDP) of the samples with different thickness, sample A: 50 Å, sample B: 80 Å, and sample C: 120 Å. The arrows indicate the interface of the $\text{LaAlO}_3/\text{La}_x\text{Al}_y\text{O}_z\text{Si}$.

instead of oxygen diffusion. When the Si species diffuse to the front of the SiO_x layer, there is no adequate oxygen environment to form the SiO_x structure; hence the Si species diffuse further into the $LaAlO_3$ film to form the $La_xAl_yO_zSi$ component. Because La_2O_3 reacts more easily with Si than Al_2O_3 does,[14] the $La_xAl_yO_zSi$ layer is rich in La.

(3) The electron density of $LaAlO_3$ layer is highly inhomogeneous and shows a graded distribution along the growth direction at the start stage of deposition. With the continuing deposition, the La and Al in the $LaAlO_3$ layer would have enough time to diffuse, therefore the compositional grade of the $LaAlO_3$ layer is decreased gradually, and eventually the $LaAlO_3$ film becomes homogeneous and compact.

ACKNOWLEDGMENT

[1]D. A. Muller, T. Sorsch, S. Moccio, F. H. Baumann, and G. Timp, Nature (London) **399**, 758 (1999).

[2]E. P. Gusev, M. Copel, E. Cartier, I. J. R. Baumvol, C. Krug, and M. A. Gribelyuk, Appl. Phys. Lett. **76**, 176 (2000).

[3]K. J. Hubbard and D. G. Schlom, J. Mater. Res. **11**, 2757 (1996).

[4]M. Copel, M. Gribelyuk, and E. Gusev, Appl. Phys. Lett. **76**, 436 (2000).

[5]H. Lee, L. Kang, R. Nieh, W. J. Qi, and J. C. Lee, Appl. Phys. Lett. **76**, 1926 (2000).

[6]M. H. Choa *et al.*, Appl. Phys. Lett. **83**, 4758 (2000).

[7]D. G. Schlom and J. H. Haeni, MRS Bull. **27**, 198 (2002).

[8]B. E. Park and H. Ishiwara, Appl. Phys. Lett. **82**, 1197 (2003).

[9]S. Stemmer, J. P. Maria, and A. L. Kingon, Appl. Phys. Lett. **79**, 102 (2001).

[10]T. Gougousi, M. J. Kelly, D. B. Terry, and G. N. Parsons, J. Appl. Phys. **93**, 1691 (2003).

[11]M. Copel, E. Cartier, and F. M. Ross, Appl. Phys. Lett. **78**, 1607 (2001).

[12]M. Gurvitch, L. Manchanda, and J. M. Gibson, Appl. Phys. Lett. **51**, 919 (1987).

[13]X. B. Lu, Z. G. Liu, Y. P. Wang, Y. Yang, X. P. Wang, H. W. Zhou, and B. Y. Nguyen, J. Appl. Phys. **94**, 1229 (2003).

[14]A. D. Li *et al.*, Appl. Phys. Lett. **83**, 3540 (2003).

[15]W. F. Xiang, H. B. Lu, L. Yan, H. Z. Guo, L. F. Liu, Y. L. Zhou, and G. Z. Yang, J. Appl. Phys. **93**, 533 (2003).

[16]V. Nitz, M. Tolan, J. P. Schlomka, O. H. Seeck, J. Stettner, and W. Press, Phys. Rev. B **54**, 5038 (1996).

[17]M. Tolan, in *X-ray Scattering from Soft-Matter Thin Films*, Springer Tracts in Modern Physics, edited by G. Hohler (Springer, New York, 1999), Vol. 148, p. 33.

[18]M. J. Guittet, J. P. Crocombette, and M. Gautier-Soyer, Phys. Rev. B **63**, 125117 (2001).

[19]T. Bekkay, E. Sacher, and A. Yelon, Surf. Sci. **217**, L377 (1989).

[20]A. Bongiomo and A. Pasquarello, Appl. Phys. Lett. **83**, 1417 (2003).

[21]S. Banerjee, S. Chakraborty, and P. T. Lai, Appl. Phys. Lett. **80**, 3075 (2002).

[22]J. H. Oh, H. W. Yeom, Y. Hagimoto, K. Ono, M. Oshima, N. Hirashita, M. Nywa, and A. Toriumi, Phys. Rev. B **63**, 205310 (2001).

[23]F. Rochet, Ch. Poncey, G. Dufour, H. Roulet, C. Guillot, and F. Sirotti, J. Non-Cryst. Solids **216**, 148 (1997).

[24]B. W. Busch, W. H. Schulte, E. Garfunkel, T. Gustafsson, W. Qi, R. Nieh, and J. Lee, Phys. Rev. B **62**, R13290 (2000).

[25]M. Copel, Appl. Phys. Lett. **82**, 1580 (2003).

[26]H. Kageshima and K. Shiraishi, Phys. Rev. Lett. **81**, 5936 (1998).

[27]G. K. Celler and L. E. Trimble, Appl. Phys. Lett. **54**, 1427 (1989).